Crystallization and Melting of Polyisoprene Rubber under Uniaxial Deformation

Yoshihisa Miyamoto,*,† Hiromi Yamao,‡ and Ken Sekimoto§

Faculty of Integrated Human Studies, Kyoto University, Kyoto 606-8501 Japan; Graduate School of Human and Environmental Studies, Kyoto University, Kyoto 606-8501 Japan; and Institut de Physique, Université Louis Pasteur, 67084 Strasbourg Cedex, France

Received March 6, 2003; Revised Manuscript Received June 16, 2003

ABSTRACT: The crystallization and the melting of vulcanized isoprene rubber under uniaxial deformation have been studied by the measurements of the stress−strain−temperature relation. The melting temperature increases approximately linearly with nominal stress for the rubbers crystallized at a fixed temperature and stress condition. It has been shown that the main origin of the rise in melting temperature with stress is the work of contraction upon melting rather than the entropy reduction on deformation in the molten state. The crystallization rate monotonically increases with nominal stress above the melting stress at a given temperature, while it shows a maximum against temperature at a given stress. The relation between the temperature and the nominal stress at the onset of crystallization is satisfactorily reproduced by the simplified kinetic model.

1. Introduction

In the study of the crystallization of polymeric materials, the investigations by introducing parameters other than temperature provide valuable information to understand the basic mechanism and useful methods to control crystallization. In the present study, the uniaxial deformation is adopted as a controlling parameter. Cross-linked rubbers are a suitable material in making use of this variable, since they easily deform up to several hundred percent and that they do not flow. Nonfluidity makes less complicated the treatment of creep under stress and allows us to determine the thermodynamic properties in the oriented molten state and the crystalline state, which are indispensable for the kinetic analysis of crystallization. The crystallization study on cross-linked rubbers conversely elucidates the thermal equilibrium range of the rubber elasticity, which is a fundamental problem in polymer physics. Further, insight into the role of the macro-Brownian movement in the polymer crystallization would be given by comparing the nucleation rate and the growth rate between the cross-linked and the un-cross-linked rubbers, though it is beyond the scope of the present paper.

The crystallization of vulcanized rubber has been studied for years and recently reported are the observations of the crystallization and the melting on deformation by the stress[1] and by the X-ray measurements.[2−5] The rubbers exhibit the variations of mechanical properties characteristic of the polymeric substances, i.e., the rubber elasticity, the viscoelasticity, and the glassy properties with decreasing temperature. In the rubbery state and the viscoelastic region, stretching induces crystallization. The crystallization upon stretching leads to the crystal and amorphous composite state from the rubbery state through the supercooled liquid state, and on retraction, the stress−strain curve shows the hysteresis loop and the thermal equilibrium rubbery state is recovered after melting.[2,5,6]

The measurements on the crystallization and the melting of rubbers under uniaxial deformation have been mostly performed with the strain as a controlling parameter, such as the growth of X-ray intensity and the stress relaxation under the strain-controlled condition. Since the phase transitions are usually treated in terms of the intensive variables, the stress-controlled measurements also give fruitful information. In particular, the stress and hence the supersaturation continuously change as the crystallization proceeds at a fixed strain. Then, the resulting rubbers are composed of the crystallites crystallized under various conditions, and the interpretation of the melting behavior of such rubbers is not straightforward.

The main purpose of the present paper is to propose a new and synthetic approach to measure and to analyze the crystallization and the melting of rubber under uniaxial deformation. In the first part of the present experiments, the temperature dependence of the relation between stress and strain has been systematically measured with the rate of deformation as a parameter which changes the time scale of observation, and the results are supplemented by X-ray measurements. In the second part, the rubbers are crystallized under a fixed temperature and stress condition, and the dependence of their melting behavior on temperature and on stress is investigated. We examine the implications of the stress−strain relation on the crystallization and the melting and of its temperature dependence. Then we discuss the origin of the rise in melting temperature with stress from the experimental result on the rubbers crystallized under the fixed temperature and stress condition. Finally, the crystallization behavior observed in the stress−strain measurements as a function of temperature and rate of deformation is discussed by the kinetic analysis.

2. Experimental Section

The material used is vulcanized synthetic *cis*-1,4-polyisoprene kindly prepared by Toyo Tire & Rubber Co. Ltd. The

† Faculty of Integrated Human Studies, Kyoto University.
‡ Graduate School of Human and Environmental Studies, Kyoto University.
§ Université Louis Pasteur.
* Corresponding author: Fax (+81)75-753-6805; e-mail miyamoto@phys.h.kyoto-u.ac.jp.

10.1021/ma0342877 CCC: $25.00
Published on Web 07/23/2003

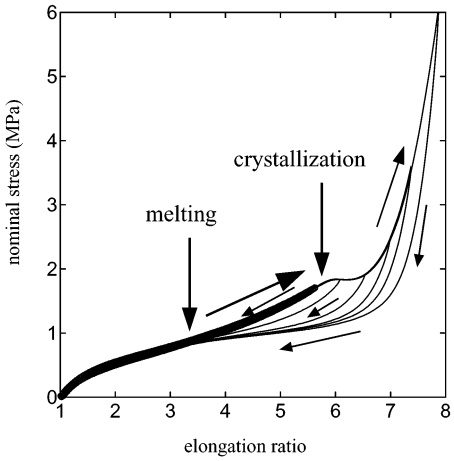

Figure 1. Maximum strain dependence of stress−strain curves at 29 °C at a rate of deformation of 0.07 s^{-1}.

composition of the rubber is zinc oxide, 1, stearic acid, 1, *n*-cyclohexyl-2-benzothiazylsulfenamide, 1, and sulfur 1.5 parts per hundred polyisoprene (IR2200, JSR). The curing condition is 160 °C for 15 min. The degree of cross-linking is estimated to be 3.8×10^{-5} mol/g from the Mooney-Rivlin elastic coefficient.

The sample dimensions used for the measurements are typically 25 mm, 5 mm, and 1 mm in the original length l_0, width w_0, and thickness d_0, respectively. The sample length l is measured by a displacement sensor and the tension f by a force gauge, and they are controlled by a pulse motor with a feedback circuit. The nominal stress is given by $\sigma = f/d_0w_0$ and the strain in terms of the elongation ratio $\lambda = l/l_0$. Most of the measurements are carried out in a temperature-controlled ethanol or water bath in order to confirm the isothermal condition, unless otherwise specified. The ranges of the temperature, T, and the rate of deformation, $\dot{\lambda}$, studied are from −60 to +80 °C and from 0.0007 to 7 s^{-1}, respectively. At low temperatures and at high $\dot{\lambda}$, the rubbers tend to break at large elongations, while at high temperatures and at low $\dot{\lambda}$ (prolonged measuring time), the effect of absorption of bath fluid is not negligible, which is examined by the reproducibility of the results: these effects limit the range of measurements.

X-ray diffraction patterns are taken by a flat camera on an imaging plate with the Cu Kα spectrum operated at 40 kV and 300 mA (Rigaku RINT2000). The exposure time was 20 min.

3. Results

3.1. Stretching and Retraction at Fixed Temperature and Rate of Deformation. We first show the stretching and retraction behavior of rubbers under a given temperature and rate of deformation condition. Figure 1 shows the maximum elongation ratio dependence of the nominal stress vs elongation ratio curve (hereafter called the stress−strain curve) at 29 °C at $\dot{\lambda} = 0.07$ s^{-1}. The rubbers are stretched up to a predetermined elongation ratio, $\lambda_{max} = 5.6$, 6.1, 6.5, 7.0, 7.4, and 7.9, and then retracted to the original length. Under the condition of $T = 29$ °C and $\dot{\lambda} = 0.07$ s^{-1}, the stretching and the retraction curves are reversible for $\lambda_{max} < 5.7$, while when $\lambda_{max} \geq 6$, they show the hysteresis, and the retraction curve almost coincides with the stretching one below $\lambda \simeq 3.1$. On retraction from $\lambda_{max} \geq 7$, the nominal stress decreases little with decreasing elongation ratio between $\lambda \simeq 6$ and $\lambda \simeq 3$, suggesting the coexistence of the crystalline and the rubbery states. This result indicates that the crystallization takes place at $\lambda \simeq 5.8$, and the melting completes at $\lambda \simeq 3.1$. When the rubber starts crystallizing at $\lambda \simeq 5.8$, the nominal stress

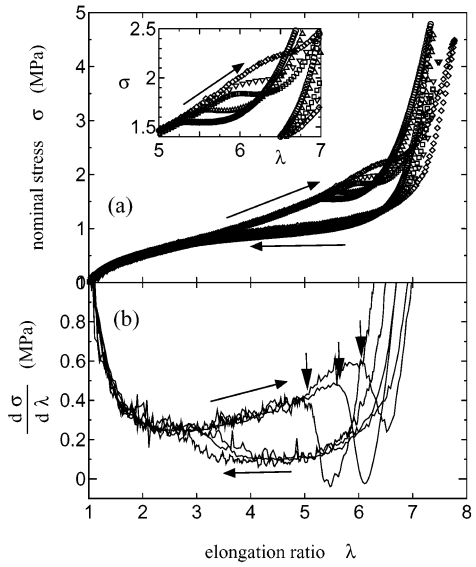

Figure 2. (a) Dependence of stress−strain curve on rate of deformation at 29 °C. The rates of deformation are (○) 0.0007, (△) 0.007, (□) 0.07, (▽) 0.7, and (◇) 7 s^{-1}. Inset: magnification in the region of the onset of crystallization. (b) Differential curves are shown for the results of $\dot{\lambda} = 0.0007$ (○), 0.07 (□), and 7 s^{-1} (◇) in (a). The vertical arrows indicate the onset of crystallization on stretching.

decreases with increasing elongation ratio (strain softening) and steeply increases at $\lambda \geq 7$ (strain hardening), which show that the rubber *elongates* on crystallization and that the rubber stiffens when crystallized.

The above interpretation of the stress−strain curve qualitatively agrees with the results of the in-situ X-ray measurements.[2,7] It is noted that in the cross-linked natural rubbers the peak or shoulder in the stress−strain curve on stretching seems less conspicuous, and the crystallization occurs at a lower elongation under a similar condition.[2,7] The latter suggests that the crystallization rate of the present synthetic rubber is smaller than that of the natural rubbers. In fact, no crystallization was observed by the X-ray measurement when the sample is stored at −25 °C for a week in the quiescent state. A brief remark concerning the stress−strain curve in the rubbery state, in the present case $\lambda \leq 3.1$, is that the stretching curve and the retraction one do not rigorously coincide at a finite deformation rate, and the small difference between them increases with decreasing temperature. This difference can be therefore attributed to the effect of viscosity of rubbers in the molten state, and we disregard this difference in the following discussion.

The dependence of stress−strain curve on rate of deformation at 29 °C is shown in Figure 2a. The elongation ratio at the onset of crystallization increases with $\dot{\lambda}$ (the inset), while that at the completion of melting is less dependent on $\dot{\lambda}$. The differential curves of Figure 2a are shown in Figure 2b for $\dot{\lambda} = 0.0007$, 0.07, and 7 s^{-1}. The elongation ratio λ_X and the nominal stress σ_X at the onset of crystallization can be unequivocally determined by a sudden decrease in $d\sigma/d\lambda$ as shown by the vertical arrows, and those at the completion of melting can be also determined by the coincidence point between the stretching and the retraction curves and slightly increase with $\dot{\lambda}$.

Figure 3 shows the temperature dependence of stress−strain curve at $\dot{\lambda} = 0.07$ s^{-1}. The elongation ratio $\lambda_f(T, \dot{\lambda})$ and the nominal stress $\sigma_f(T, \dot{\lambda})$ at the completion of

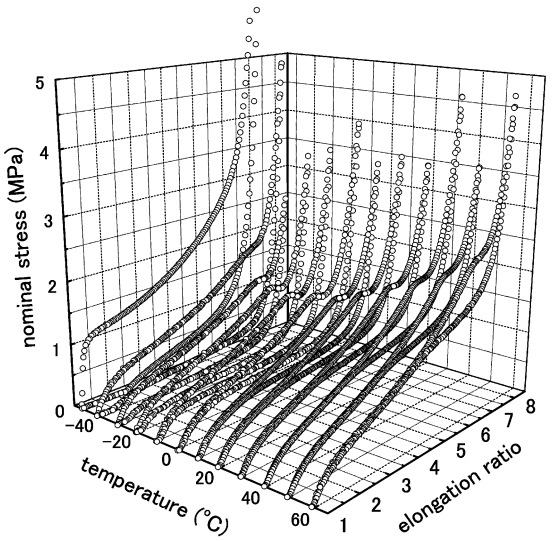

Figure 3. Temperature dependence of stress−strain curve at a rate of deformation of 0.07 s^{-1}.

melting increase with increasing temperature above 0 °C. Below −15 °C, the tension vanishes before the sample length reaches its original length l_0 on retraction, which indicates that the length of the crystallized rubber is larger than l_0 and the melting temperature in the undeformed state is higher than −15 °C. Above −10 °C, $\lambda_X(T,\dot{\lambda})$ and $\sigma_X(T,\dot{\lambda})$ at the onset of crystallization increase with increasing temperature, while they increase with decreasing temperature below −10 °C.

The relations among temperature, nominal stress, and elongation ratio at the onset of crystallization and at the completion of melting are shown in Figure 4a,b with the rate of deformation as a parameter. As a reference, the dependence of glass transition temperature T_g on nominal stress and elongation ratio[8] is also shown in the figure. For the broken and solid lines, see Figures 8−10 and the Discussion, respectively. At a given $\dot{\lambda}$, i.e., following the same symbols, $\sigma_f(T,\dot{\lambda})$ and $\lambda_f(T,\dot{\lambda})$ at melting increase with temperature, and $\sigma_X(T,\dot{\lambda})$ and $\lambda_X(T,\dot{\lambda})$ at crystallization increase with increasing temperature at high temperatures while they increase with decreasing temperature at low temperatures. At a given temperature, all these four quantities increase with $\dot{\lambda}$.

3.2. X-ray Measurements. The melting of the vulcanized isoprene rubber under strain is examined by X-ray measurements. The rubber is stretched up to a predetermined elongation ratio (λ = 4.2, 4.5, and 4.65) at room temperature in the air. Then the rubber is mounted on a metal sample holder, transferred to a refrigerator at −20 °C at the fixed length, and kept there at least for 24 h. Judging from the results shown in Figures 2 and 4, the crystallization is supposed to proceed at −20 °C rather than during the stretching or the cooling processes. X-ray diffraction patterns are taken at 5 K intervals with stepwise heating under the fixed length condition and shown in Figure 5a−c for λ = 4.65. The X-ray patterns show that the chain axis is highly oriented along the stretching direction, and the amorphous part is much less oriented.[2,5,9] The Bragg diffraction intensities decrease with increasing temperature and disappear completely at 60 °C. The variation in 200 reflection intensity with temperature is shown in Figure 5d. The intensity linearly decreases with temperature, and the melting temperature $T_f(\lambda)$ is

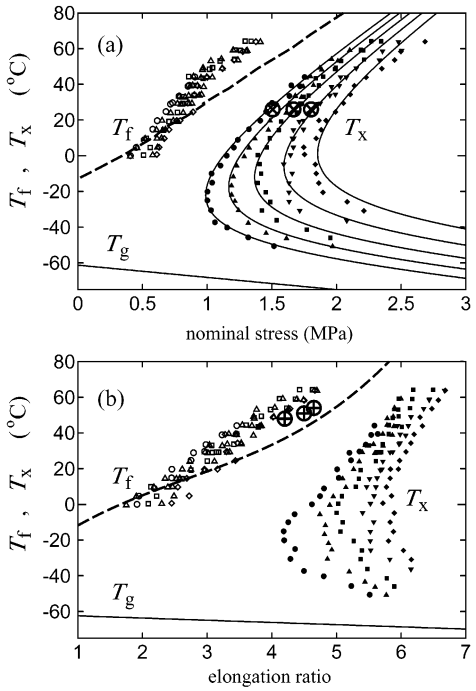

Figure 4. (a) Nominal stress and (b) elongation ratio dependence of crystallization T_X and melting T_f temperatures determined by the stretching and retraction measurements under the constant rate of deformation. The rates of deformation are (○) 0.0007, (△) 0.007, (□) 0.07, (▽) 0.7, and (◇) 7 s^{-1}. Open symbols show the melting temperatures, and closed ones show the crystallization temperatures. The glass transition temperature T_g is also shown.[8] The broken lines indicate the melting temperature of the rubbers crystallized under the fixed temperature and nominal stress condition shown in Figure 10. (a) ⊗: The crystallization conditions of temperature and nominal stress shown in Figure 6. (b) ⊕: The melting temperature determined by the X-ray measurements (Figure 5). The solid lines in (a) show the contour lines of crystallization rates corresponding to $\dot{\lambda}$ from 0.0007 to 7 s^{-1} from left to right, deduced from Figure 13 and eqs 7−9.

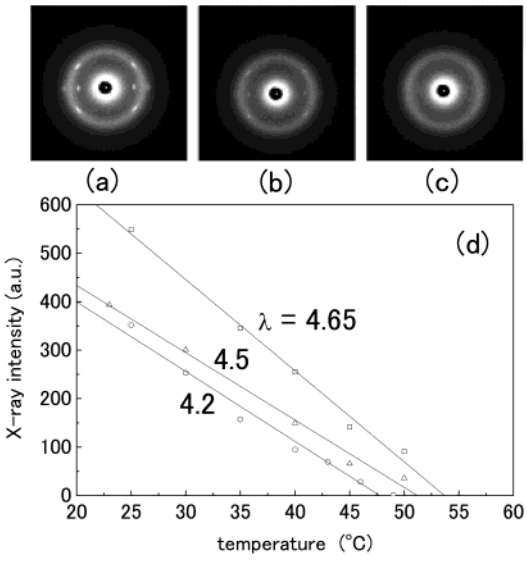

Figure 5. Change in X-ray pattern with increasing temperature at an elongation ratio of 4.65: (a) 25, (b) 45, and (c) 60 °C. The stretching direction is vertical. (d) Temperature dependence of the 200 reflection intensity on heating at elongation ratios 4.2, 4.5, and 4.65.

determined by the temperature at which the Bragg intensity disappears, shown in Figure 4b (⊕). The melting temperatures determined by the X-ray mea-

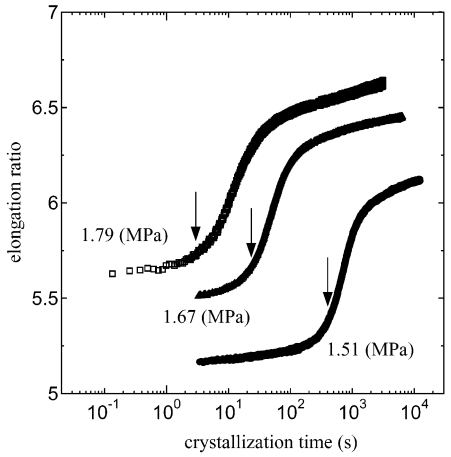

Figure 6. Crystallization time dependence of elongation ratio at $\sigma_X = 1.51$ (○), 1.67 (△), and 1.79 MPa (◇) at $T_X = 26$ °C. The arrows indicate the time corresponding to $(\dot{\lambda}(T_X,\sigma_X))^{-1}$ estimated from the crystallization condition (⊗) in Figure 4.

surements approximately agree with those determined by the stress−strain curves.

3.3. Melting of Rubbers Crystallized at Fixed Temperature and Stress. The dependence of T_X on the rate of deformation in Figure 4 indicates that the crystallization is a kinetic process, while that of T_f may be due to either the melting dynamics or the variation in the melting point of the crystals crystallized under different crystallization conditions. The stress at melting $\sigma_f(T,\dot{\lambda})$ is that of the crystal formed at $\sigma_X(T,\dot{\lambda})$ on stretching. At a given T, therefore, the rubber stretched at a larger $\dot{\lambda}$ crystallizes at a larger σ, i.e., at a larger supersaturation. To clarify the above issue, the melting behavior of the crystals crystallized under a fixed temperature and nominal stress condition is examined.

In the supersaturated state, the stress relaxes if the length of the rubber is fixed,[1,10,11] and the rubber elongates if the tension is fixed. The change in elongation ratio with time when the nominal stress is kept constant at 26 °C is shown in Figure 6. The rubber is stretched at $\dot{\lambda} = 7$ s^{-1} up to a given nominal stress (e.g., along the solid line in Figure 7a up to $\sigma = 1.8$ MPa), and the elongation of rubber is measured during crystallization at the fixed nominal stress. Figure 6 shows that the rubbers elongate upon crystallization and that the elongation ratio exhibits the sigmoidal curve typical to crystallization, indicating that the primary crystallization is completed within the crystallization time elapsed, with further gradual elongation at prolonged time. The half-time of crystallization is 660 s at 1.51 MPa, 44 s at 1.67 MPa, and 11 s at 1.79 MPa, and the corresponding crystallization conditions are shown in Figure 4a by crossed circles (⊗).

The melting behavior of the crystals crystallized at the condition corresponding to the leftmost curve in Figure 6 is studied. Crystallization is carried out before each melting scan in a total of 30 times. In these 30 crystallizations, the crystallization condition is as follows: the temperature is $T_X = 26 \pm 1$ °C, the nominal stress, $\sigma_X = 1.80 \pm 0.03$ MPa, and the crystallization time, 3100 ± 100 s. The elongation ratio changes upon crystallization from 5.7 ± 0.1 to $\lambda_{fin} = 6.7 \pm 0.1$ as shown by a thick arrow in Figure 7a, and the half-time of crystallization is 10.0 ± 3.8 s. These crystallizations are carried out in the air in order to transfer the rubbers rapidly to the temperature and/or the nominal stress for the subsequent melting measurements.

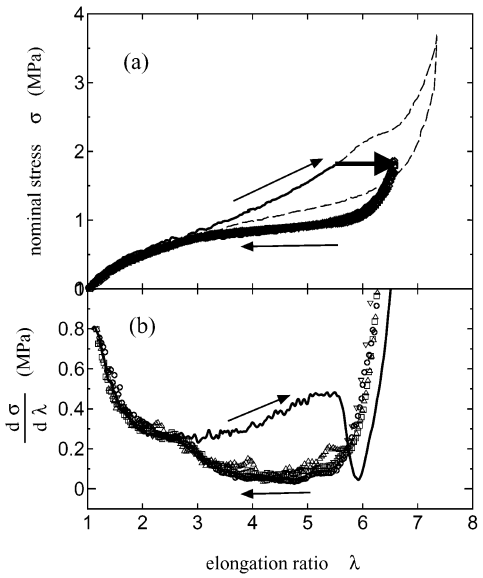

Figure 7. (a) Contraction curves at 26 °C at various contraction rates after crystallized at $\sigma_X = 1.8$ MPa and $T_X = 26$ °C and (b) their differential curves. The contraction rates are (○) 0.0007, (△) 0.007, (□) 0.07, (▽) 0.7, and (◇) 7 s^{-1}. (a) The solid and broken curve represents the stress−strain curve at 26 °C at $\dot{\lambda} = 7$ s^{-1}. The rubbers are stretched along the solid curve up to 1.8 MPa at 26 °C, and then the stress is maintained. The thick arrow indicates the elongation of rubbers during crystallization at $\sigma_X = 1.8$ MPa. (b) Differential curve on stretching at 26 °C at $\dot{\lambda} = 0.07$ s^{-1} is shown by a solid line for comparison.

The dependence of the contraction curve on rate of deformation at 26 °C after the crystallization and its differential curve are shown in parts a and b of Figure 7, respectively. Since the results in Figure 7a,b clearly show that the contraction curves are independent of $\dot{\lambda}$, it is concluded that the origin of the dependence of melting on rate of deformation observed in Figures 2 and 4 is the difference in the crystallization conditions.

The relation between the temperature and the nominal stress at melting is measured by the following complementary methods: the heating at constant nominal stress which gives the nominal stress dependence of the melting temperature, $T_f(\sigma)$, and the contraction at constant temperature, $\sigma_f(T)$.

The experimental procedure of the first method is as follows. After the crystallization under the above condition, the rubbers are quenched to −20 °C at the fixed length λ_{fin}, and a prescribed nominal stress is given. They are further cooled to −50 °C, and then the change in elongation ratio is measured upon heating at 1 K/min under the fixed stress condition. In this procedure, the choice of the quenching temperature of −20 °C is arbitrary so far as it is well below the melting temperature in the unstrained state (the quenching temperature was examined in the range between −20 and −40 °C) and did not affect the results shown below. The change in nominal stress for $T < T_X$ on cooling and heating at a fixed elongation ratio of $\lambda_{fin} = 6.7$ is reversible with the temperature coefficient larger than the proportionality to the absolute temperature.

The heating curves under various fixed nominal stresses are shown in Figure 8a. The shrinkage of the rubber is observed in a narrow range of temperatures. At the higher temperatures, the elongation ratio decreases approximately proportional to the reciprocal absolute temperature, characteristic of the rubbery

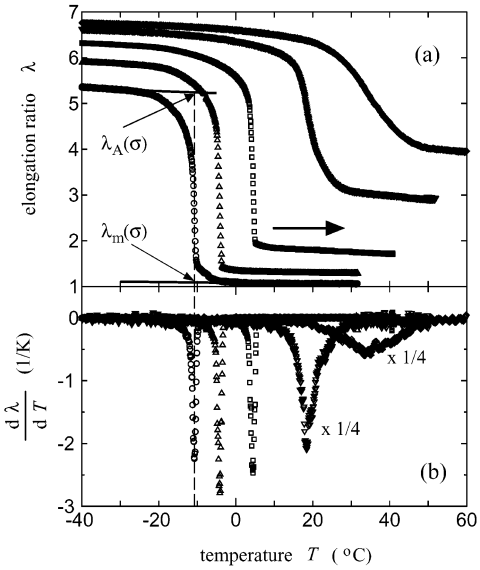

Figure 8. (a) Change in elongation ratio on heating at 1 K/min at various nominal stress after crystallized at $\sigma_X = 1.8$ MPa and $T_X = 26$ °C and (b) the differential curves: (○) 0.036, (△) 0.18, (□) 0.42, (▽) 0.68, and (◊) 1.11 MPa. (a) The solid curves are the elongation ratios extrapolated from low (linear in T) and high (proportional to T^{-1}) temperature for $\sigma = 0.036$ MPa.

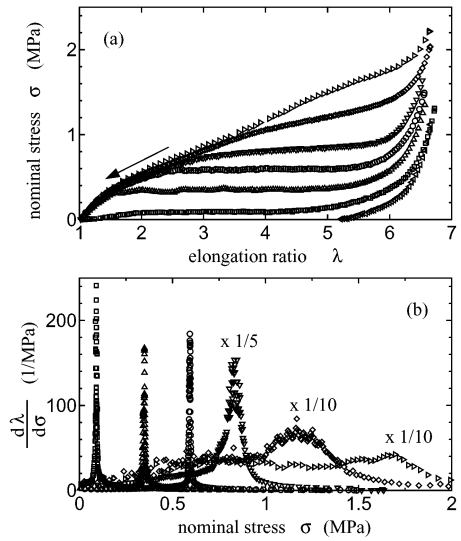

Figure 9. (a) Contraction curves at various temperatures after crystallized at $\sigma_X = 1.8$ MPa and $T_X = 26$ °C. (b) Differential curves of elongation ratio with respect to nominal stress. (left-tilted △) −20.5, (□) −10.2, (△) −0.5, (○) 9.7, (▽) 19.6, (◊) 39.3, and (right-tilted △) 58.5 °C.

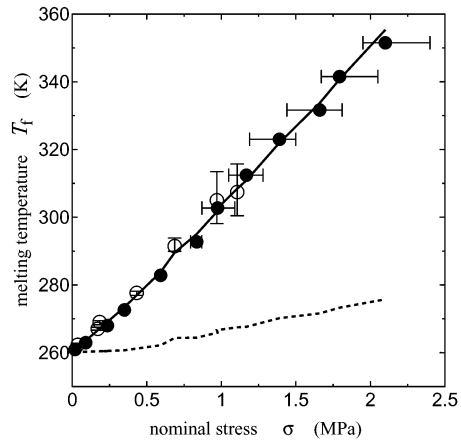

Figure 10. (a) Relation between the temperature and the nominal stress at melting determined by the heating (○, Figure 8) and by the contraction measurements (●, Figure 9). The broken line shows the nominal stress dependence of melting temperature calculated by eq 3, and the solid line shows that by eq 6 with $\Delta\lambda_f = -8.9$. The vertical and horizontal bars indicate the range of melting determined by the half-width of the peaks in Figures 8b and 9b, respectively.

state, which reconfirms the sharp drop in elongation ratio is due to melting. The differential curves of Figure 8a are shown in Figure 8b: the melting temperature at a given nominal stress $T_f(\sigma)$ can be clearly identified from the sharp peak in the differential curves. Note that the melting temperature thus determined is the one at which the crystals melt most, while that determined from Figures 2 and 3 and shown in Figure 4 is the temperature at which the final trace of crystal disappears. The temperature range of shrinkage increases with increasing melting temperature, in particular, at $T_f(\sigma) > T_X = 26$ °C.

In the second method, the rubbers crystallized at $\sigma_X = 1.8$ MPa and $T_X = 26$ °C are transferred at the fixed $\lambda_{fin} \simeq 6.7$ to a temperature of the contraction curve measurement, and the tension is measured on contraction at $\dot{\lambda} = 0.07$ or 0.7 s^{-1}. Figure 9a shows the stress−strain curves on contraction from $\lambda_{fin} \simeq 6.7$. Since the stress-controlled measurements give almost the same results and the measurements at constant $\dot{\lambda}$ are experimentally more stable and accurate, the stress on contraction at constant $\dot{\lambda}$ was measured in the second method. Below −15 °C, the tension vanishes at $\lambda > 1$, similar to Figure 3. At -12.5 °C $< T < T_X = 26$ °C, fairly constant stress is observed during contraction, while at higher temperatures ($T > T_X$) the nominal stress continuously decreases on contraction. In both cases, $\sigma(\lambda,T)$ shows the values in the rubbery state when $\sigma < \sigma_f(T)$. The differential curves of elongation ratio with respect to nominal stress, $(d\lambda/d\sigma)(\sigma)$, is shown in Figure 9b. The nominal stress at melting at a given temperature $\sigma_f(T)$ is determined by the peak position in Figure 9b.

The relation between the temperature and the nominal stress at melting, $f_{coexist}(T_f,\sigma_f) = 0$, determined from Figures 8b and 9b is shown in Figure 10. The results obtained by the heating (closed circles) and by the contraction measurements (open circles) agree well with each other. The results are also shown in Figure 4 by the broken lines. The melting temperature as a whole linearly increases with nominal stress including $T_f(\sigma_f) > T_X = 26$ °C and is expressed by $T_f = 259 + 45\sigma_f$ K (σ_f in MPa). At small nominal stresses, the slope of the curve slightly decreases, and a closer look reveals $T_f(\sigma_f \to 0) \simeq -13$ °C $= 260$ K.

At the end of this section, a remark is made on the homogeneity of deformation. The deformation of rubber is macroscopically homogeneous in most measurements of the present study. In some cases, however, the deformation becomes macroscopically inhomogeneous, in which the width and the thickness of rubber vary along the specimen; that is, single or multiple thicker parts and thinner parts coexist under the common tension, suggesting that the thicker parts are in the molten state and the thinner ones in the crystallized state. The inhomogeneous deformation is observed at a small strain at a slow ramping rate in the melting process, for example, in the retraction in the stress−strain curve measurements around −5 °C at $\dot{\lambda} = 0.0007$

s^{-1}, in the heating measurement at $\sigma = 0.036$ MPa around -10 °C (Figure 8), etc. Details are under investigation.

4. Discussion

In the crystallization of polymer networks from the stretched state, two types of mechanisms are proposed: the stress-induced crystallization and the temperature-induced crystallization.[12] When the rubbers are stretched at a temperature up to an elongation ratio at which the melting temperature is higher than the ambient temperature, the stress-induced crystallization occurs. After the stress relaxation by crystallization, further crystallization, i.e., the temperature-induced crystallization, takes place when the temperature is lowered. If the average strain in the molten rubbery region can be assumed to be given by the stress at a given temperature, the stress relaxation by crystallization implies that the strain in the rubbery region and hence the supersaturation decrease as the crystallization proceeds. At the end of stress relaxation, the crystallization rate becomes small or may be even zero, and the primary crystallization may not be completed in the stretched state depending on the initial conditions of the temperature and the elongation ratio. On cooling from this state, the further primary crystallization may well take place as well as the secondary crystallization. Here, the primary crystallization refers to the space-filling process of polycrystalline aggregates, and the secondary crystallization refers to the crystallization and the reorganization processes after the primary crystallization. When the samples are brought into the state of a larger supersaturation after the primary crystallization, less stable crystallites are formed, which melt at lower temperatures,[14] and when heated, the annealing effect involves the reorganization or the recrystallization which leads to more stable crystallites with higher melting temperatures.

On the other hand, when the nominal stress and the temperature are maintained during crystallization, the supersaturation remains approximately constant, apart from the change in true stress. Figure 6 indicates that the primary crystallization is completed with an effect of the secondary crystallization at prolonged time under the present crystallization condition. Then on quenching the samples into a state of larger supersaturation of -20 °C at a fixed length, λ_{fin}, the temperature-induced crystallization may take place as the further secondary crystallization.

Since the relations $\sigma(\lambda,T)$ for $T > T_f$ in Figure 8a and for $\sigma < \sigma_f$ in Figure 9a correspond to that in the rubbery state, the peaks observed in Figures 8b and 9b indicate the melting of the crystallites into the rubbery state.

We discuss the effect of the secondary crystallization at $T < T_X$. Despite the possible existence of the temperature-induced crystallites, the present measurements can be considered to determine the melting point of the stress-induced crystallites formed at σ_X and T_X for the following reasons. In other words, the present method of measurement may be insensitive to the melting of the temperature-induced crystallites formed by the secondary crystallization. First, the crystallization rate of the present material is much smaller than the natural rubbers (NR) as noted in Results section, suggesting the contribution of the temperature-induced crystallites is accordingly small. Second, the melting behavior observed by the first method of the heating under the fixed stress does not depend on the quenching temperature, which is arbitrarily chosen as -20 °C in the present set of measurements. Third, the change in $\sigma(\lambda_{fin},T)$ on cooling and heating after the crystallization is reversible in the range $T < T_X$. These results show that the effect of the temperature-induced crystallites is relatively small on the basic amorphous and crystal composite structure formed under the present crystallization conditions. At the same time, however, the reversible change in $\sigma(\lambda_{fin},T)$ and its large temperature dependence suggest that the cooling and heating affect, though small, the composite structure in a reversible manner for $T < T_X$: these observations may be relevant to the approximately reversible change in the lamellar structure observed in NR.[13]

The effect of annealing can be seen for $T_f(\sigma_f) > T_X$ in the increase in the temperature and the stress ranges of shrinkage with increasing T_f, as shown in Figures 8 and 9, respectively, and also in Figure 10. Though the melting temperature will increase and the melting stress will decrease by the annealing effect, Figure 10 shows that the corrections for σ_f and T_f determined by the peak positions are not important.

We have obtained from the above experiments (1) the equation of state in the rubbery state, $f_{stateR}(T,\sigma,\lambda_R) = 0$, where λ_R is the elongation ratio in the rubbery state (e.g., Figure 3), (2) the relation at the onset of crystallization, $f_{onset}(T_X,\sigma_X,\dot{\lambda}) = 0$ (Figure 4a), and (3) the coexistence condition of the melt and the crystal of the rubbers crystallized at 1.8 MPa and 26 °C, $f_{coexist}(T_f,\sigma_f) = 0$ (Figure 10). In this section we will discuss the rise in melting temperature with stress from the viewpoint of the entropy reduction upon deformation and from the thermodynamics under uniaxial extension and the crystallization kinetics by a simplified treatment.

The crystallites grown under the above crystallization condition should be of finite size, and hence the melting temperature shown in Figure 10 is not the equilibrium melting temperature. The crystallization rate strikingly decreases with increasing cross-linking for NR and is much faster in NR than in synthetic isoprene rubber (IR).[1,10,15,16] Also known is the large effect of fatty acids on the nucleation process of NR.[17,18] On the other hand, the observed melting temperature for the rubbers crystallized under similar conditions is little affected by the cross-linking for NR and is similar between NR and IR or somewhat higher for NR than IR.[1,15] In the unstrained state of an unvulcanized NR, the equilibrium melting temperature is experimentally determined to be 35.5 °C by extrapolating the observed melting temperature to the infinite lamellar thickness.[19] It is therefore expected that the equilibrium melting temperature in the unstrained state $T_f^0(\sigma_f = 0)$ of the present material is similar to that of unvulcanized NR, about 35.5 °C (or somewhat lower), higher by nearly 50 K than the observed $T_f(\sigma_f = 0) \simeq -13$ °C.

We proceed with the discussion on the melting temperature rise with stress based on the observed $f_{coexist}(T_f,\sigma_f) = 0$ because we are concerned with the change in $T_f(\sigma_f)$ with σ_f but not with the absolute value of $T_f^0(\sigma_f^0)$. We will take the difference between T_f and T_f^0 into account in estimating the supersaturation in the subsequent discussion about crystallization. In addition, the heat of fusion in the unstrained state, $\Delta h_f(\sigma = 0)$, is assumed to be 64 MJ/m^3 as a reference value, which is the value for unvulcanized natural rubber.[20,21] The following discussions are qualitatively insensitive to the

choice of the $\Delta h_f(\sigma = 0)$ value, but the numerical values given below depend on them.

4.1. Melting. It is well-known that the melting temperature increases when polymeric substances are subjected under strain, and the rise in melting temperature is in general attributed to the reduction of the entropy in the molten state. In this case, it is implicitly assumed that the change in enthalpy and entropy in the crystalline state can be neglected. We first examine whether the above idea is applicable to the present experimental result.

The basic thermodynamic relation for the rubber under strain is given by $du = T\,ds - p\,dv + \sigma\,d\lambda$, where p is the hydrostatic pressure and u, s, and v are the internal energy, the entropy, and the volume of the system, respectively. The enthalpy $\hat{h}$ is defined by $\hat{h} \equiv u + pv$, and the enthalpy under stress is defined by $dh \equiv d(\hat{h} - \sigma(\lambda - 1)) = T\,ds - (\lambda - 1)\,d\sigma$, as the pressure remains unchanged in the present study. The Helmholtz free energy $f_j \equiv \hat{h}_j - Ts_j$ and the Gibbs free energy $g_j \equiv h_j - Ts_j$ are defined in the ordinary way, where the subscript $j =$ "R" stands for the rubbery state and $j =$ "c" for the crystalline state. Since the tensile force, or the nominal stress, is common between the melt and the crystal in the coexistence state, the melting temperature T_f at the nominal stress σ_f is given by

$$T_f(\sigma_f) = \frac{\Delta h_f(\sigma_f)}{\Delta s_f(\sigma_f)} = \frac{\Delta \hat{h}_f - \sigma_f \Delta \lambda_f}{\Delta s_f} \tag{1}$$

where Δx_f signifies the difference in the quantity x between the molten and the crystalline states at the melting point (T_f,σ_f), for example, $\Delta s_f(\sigma_f) \equiv s_R(T_f,\sigma_f) - s_c(T_f,\sigma_f)$.

The change in entropy in the rubbery state on deformation can be obtained from the equation of state, $f_{stateR}(T,\sigma,\lambda_R) = 0$. Here we calculate the change in Helmholtz free energy per unit volume according to the Mooney's method:[6]

$$f_R(T,\lambda_R) - f_R(T,1) = C_1(I_1 - 3) + C_2(I_2 - 3) \tag{2}$$

where I_1 and I_2 are the strain invariants, and $I_1 = \lambda_R^2 + 2\lambda_R^{-1}$ and $I_2 = 2\lambda_R + \lambda_R^{-2}$ in the case of uniaxial extension. The coefficients C_1 and C_2 are determined from the intercept and the slope in the Mooney plot, $\sigma/2(\lambda_R - \lambda_R^{-2})$ vs λ_R^{-1}, respectively. In the Mooney plot at a given temperature T, the experimental result $\sigma(T,\lambda_R)$ on stretching and below $\sigma_f(T)$ is employed. The temperature dependence of C_1 (closed symbols) and C_2 (open symbols) is shown in Figure 11. In the figure, the results at $\dot{\lambda}$ smaller than 0.07 s^{-1} are shown, but those for higher $\dot{\lambda}$ are almost the same. The linear regressions give $C_1 = 0.77 \times 10^{-4} + 3.1 \times 10^{-4}T$ MPa and $C_2 = 0.11 + 2.5 \times 10^{-5}T$ MPa and are shown in Figure 11 by a solid line for C_1 and a broken line for C_2. The coefficient C_1 is approximately proportional to the absolute temperature T, and the C_2 term is independent of T.[22] When we assume that the temperature derivative of σ is the change in entropy on extension and that the temperature independent σ is the change in energy, the results suggest that the C_1 term is of the entropic origin and C_2 of the energetic origin, though the scatter of the data prevents us from drawing the definite conclusion.[23]

If the increase in melting temperature from $T_f(\sigma_f = 0)$ is assumed to arise only from the contributuion of the rubber elasticity, the melting temperature at σ_f is expressed by

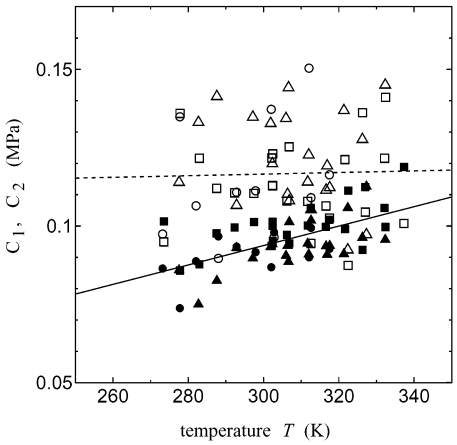

Figure 11. Temperature dependence of the Mooney coefficients: (○) $\dot{\lambda} = 0.0007$, (△) 0.007, and (□) 0.07 s^{-1}. The filled symbols are for C_1, and the open ones are for C_2.

$$T_f(\sigma_f) = \frac{\Delta h_f(0) + C_2(I_2(\lambda_m(\sigma_f)) - 3)}{\Delta s_f(0) - C_1'(I_1(\lambda_m(\sigma_f)) - 3)} \tag{3}$$

where $C_1' = C_1/T$ and $\lambda_m(\sigma_f) \equiv \lambda_R(T_f,\sigma_f)$. The result calculated by eq 3 is shown in Figure 10 by a broken line, with the approximations $C_1' = C_1/T = 3.1 \times 10^{-4}$ MPa/K, which gives the cross-link density of 3.8×10^{-5} mol/g, $C_2 = 0.11$ MPa, and $T_f(\sigma_f = 0) = 260$ K. The result shows that the change in free energy in the rubbery state by elongation accounts for at most one-sixth of the observed increase in melting temperature with nominal stress. Even when it is assumed that the stress at room temperature is totally of the entropic origin,[24] the similar increase in T_f results as has been pointed out.[11,25] From these results, the contribution to the free energy from the rubber elasticity is found to be not enough to explain the observed rise in melting temperature with stress.

The factor overlooked in the above discussion is the work of contracting the length of the system in the crystalline state to that in the molten state under the external tensile force or, equivalently, that of elongation upon crystallization, $-\sigma_f\Delta\lambda_f$, appeared in the numerator in eq 1. Note that $\Delta\lambda_f \equiv \lambda_R(T_f,\sigma_f) - \lambda_c(T_f,\sigma_f) < 0$ as the rubber shrinks on melting and that λ_c is defined by the ratio of the length of the system in the crystalline state to the natural length in the rubbery state. The value of $\Delta\lambda_f$ can be estimated from the Clapeyron−Clausius relation

$$\frac{dT_f}{d\sigma_f} = \frac{-\Delta\lambda_f(T_f,\sigma_f)}{\Delta s_f(T_f,\sigma_f)} = \frac{-T_f\Delta\lambda_f}{\Delta\hat{h}_f - \sigma_f\Delta\lambda_f} \tag{4}$$

When it is assumed that $\Delta\hat{h}_f$ is constant and given by $\Delta h_f(0) = 64$ MJ/m^3, disregarding the rubber elasticity contribution, and that the relation is linear between T_f and σ_f, then Δs_f and $\Delta\lambda_f$ are found to be both constant and given by

$$\Delta s_f = \frac{\Delta\hat{h}_f}{T_f(0)} \quad \text{and} \quad \Delta\lambda_f = \frac{\Delta\hat{h}_f}{T_f(0)}\frac{dT_f}{d\sigma_f} \tag{5}$$

leading to $\Delta s_f = 0.25$ MJ/(m^3 K) and $\Delta\lambda_f = -11$.

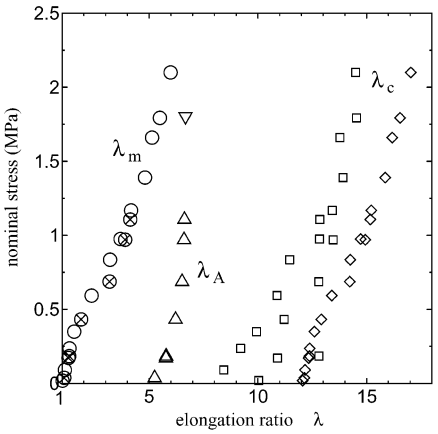

Figure 12. Relation between the nominal stress and the elongation ratio along the coexistence line shown in Figure 10. The elongation ratio of the melt determined by the contraction (○, Figure 9) and the heating measurements (⊗, Figure 8) and that of the crystal calculated by eq 5 (◇) and from eq 6 (□) with $\lambda_c = \lambda_m - \Delta\lambda_f$. The elongation ratio of the rubbers crystallized at $\sigma_X = 1.8$ MPa and $T_X = 26$ °C just after crystallization (λ_{fin}: ▽) and at melting in Figure 8 (λ_A: △).

When the work of contraction on melting is not negligible and the contributions from the rubber elasticity are taken into account, $T_f(\sigma_f)$ is given by the following equation from eq 1 instead of eq 3:

$$T_f(\sigma_f) = \frac{\Delta h_f(0) + C_2(I_2(\lambda_m) - 3) - \sigma_f \Delta\lambda_f}{\Delta s_f(0) - C_1'(I_1(\lambda_m)) - 3)} \qquad (6)$$

From the observed $T_f(\sigma_f)$, $\Delta\lambda_f$ can be calculated by eq 6 (see Figure 12) and found to be about −9, approximately independent of σ_f. In fact, eq 6 with $\Delta\lambda_f = -8.9$ gives an excellent fit to the observed melting temperature as shown in Figure 10 by a solid line. From this result, the major factor controlling the rise in melting temperature with stress can be attributed to the work of contraction upon melting. It may be worth noting that the elongation upon crystallization plays a role not only in the crystallization of rubbers under strain but also of polymeric substances in general, even in the quiescent state. The above conclusion may be specific to a group of polymers because fair agreement in the melting temperature rise with strain is observed between the measurements and the theory for cross-linked *trans*-polychloroprene and *trans*-polyisoprene,[26−29] where the melting temperature rise is much smaller (ca. 15 and 5 K for $\lambda = 4$) than the present result (ca. 50 K for $\lambda = 4$).

4.2. Crystallization. Next, the structure developing during the crystallization is discussed. The elongation ratio in the crystalline state at melting point, $\lambda_c(T_f,\sigma_f)$, which corresponds to the equilibrium value of the fully crystalline state, is obtained by $\lambda_c = \lambda_m - \Delta\lambda_f$ by the use of eq 5 or 6. Figure 12 shows the stress dependence of λ_m and λ_c. In the figure also shown are the elongation ratio just after crystallization ($\sigma_f = 1.8$ MPa and $\lambda_{fin} = 6.7$) and that before melting at melting point, $\lambda_A(T_f,\sigma_f)$, determined by the elongation ratio of the crystallized state extrapolated to the melting temperature in the heating experiment (Figure 8). The intermediate value of λ_A between λ_m and λ_c indicates that the crystallized rubber has limited crystallinity. This result and the sigmoidal crystallization curve in Figure 6 suggest that the aggregates composed of nearly constant amorphous and crystal structure increase their fraction with crystallization time, presumably by the nucleation and growth, analogous to the spherulitic growth in the quiescent state. The stress relaxation and the elongation in the rubbers on crystallization imply that the crystallites and the amorphous region are primarily arranged in series in the aggregate, and the crystallites are supposed to be the lamellar crystals with the chain axis parallel to the stretching direction.[13] The formation of a fiberlike crystal will hardly lead to the elongation of the rubber under a given stress nor to the relaxation of stress at a given strain; the present method of measurement is insensitive to the formation of the fiberlike crystal or of the "shish".

The simple series model is, however, quite unsatisfactory for explaining the experimental results quantitatively. The simple series model would give a constant value for a measure of the crystallinity $(\lambda_{fin} - \lambda_m)/\Delta\lambda_f = (\lambda_A - \lambda_m)/\Delta\lambda_f$, while in Figure 12, $(\lambda_{fin} - \lambda_m)/\Delta\lambda_f$ is about 0.1 just after the crystallization, but $(\lambda_A - \lambda_m)/\Delta\lambda_f$ increases up to about 0.5 with decreasing σ_f (or T_f). We should construct models including the aspects of transversal interaction among the hard domains mediated by the elasticity of soft domains.

The σ_f dependence of λ_c in Figure 12 is puzzling as well. Since Young's modulus in the crystalline state (∼1 GPa) should be much larger than that in the rubbery state (≃1 MPa), and that the linear thermal expansion coefficient of the former would be of the same order and smaller than that of the latter ($\sim 10^{-4}$ K^{-1}), the σ_f dependence of λ_c is expected to be much smaller than that of λ_m, in contrast to the result shown in Figure 12. Further investigations will be necessary in regard to the elastic and thermal properties of the crystallized rubbers and the σ_f (or T_f) dependence of $\Delta\lambda_f$. The assumption that λ_c = constant is another possibility instead of that $\Delta\hat{h}_f = \Delta h_f(0)$ = constant. In this case, however, the thermodynamic arguments result in a marked decrease in both $\Delta\hat{h}_f$ and Δh_f with σ_f (or T_f), which is considered unlikely.

Finally, we will examine the relation at the onset of crystallization, $f_{onset}(T_X,\sigma_X,\dot{\lambda}) = 0$ in Figure 4a. This relation signifies the condition (T_X,σ_X) under which the crystallization is observable at the time scale of the order of reciprocal of $\dot{\lambda}$. In other words, when the crystallization rate at the onset, $\dot{X}_{onset}$, is expressed as a function of temperature and nominal stress, the condition (T_X,σ_X) at a given $\dot{\lambda}$ corresponds a contour line of $\dot{X}_{onset}(T_X,\sigma_X)$. Therefore, Figure 4a shows that at a fixed σ the crystallization rate increases with increasing supercooling (decreasing temperature), passes through a maximum, and then decreases with supercooling on approaching to the glass transition temperature; that is, the observed $f_{onset}(T_X,\sigma_X,\dot{\lambda}) = 0$ shows a bell-shaped temperature dependence of the crystallization rate as often observed in polymeric materials.

Since $\dot{\lambda}(T_X,\sigma_X)$, which is another way of writing the relation $f_{onset}(T_X,\sigma_X,\dot{\lambda}) = 0$, and $\dot{X}_{onset}(T_X,\sigma_X)$ should be proportional to each other with a proportionality coefficient of the order of unity, these quantities are equated in the following analysis. From the crystallization conditions at fixed (T_X,σ_X) of Figure 6, shown in Figure 4a by crossed circles (⊗), the corresponding $\dot{\lambda}(T_X,\sigma_X)$ can be estimated by the interpolation in Figure 4a. The reciprocal of the estimated $\dot{\lambda}(T_X,\sigma_X)$ is shown in Figure 6 by the vertical arrows. This result indicates $\sigma_X(T_X,\dot{\lambda})$ in fact shows the condition at the onset of crystallization at the time scale of $\dot{\lambda}^{-1}$.

The crystallization rate $\dot{X}$ at (T_X,σ_X) is determined by the transport factor $\phi(T_X,\sigma_X)$ and the kinetic factor $\kappa(T_X,\sigma_X)$. The kinetic factor depends on the nucleation rate and the growth rate of crystal. In the case of polymeric materials, the growth rate is expressed, even at large supercoolings, by the "nucleation type" temperature dependence[30−32] rather than by the Wilson formula,[33] and the transport factor is expressed by the Vogel−Fulcher (VF) equation or the Williams−Landel−Ferry (WLF) equation.[34] In the present analyses, it is assumed that the supersaturation dependence of crystallization rate at the onset of crystallization is dominated either by the nucleation rate or by the growth rate:

$$\dot{X}_{onset}(T_X,\sigma_X) = \dot{X}_0^{(i)}\phi(T_X,\sigma_X)\,\kappa^{(i)}(T_X,\sigma_X) \qquad (7)$$

where $\dot{X}_0^{(i)}$ is a constant and

$$\kappa^{(i)}(T_X,\sigma_X) = \exp\left(-\frac{K^{(i)}}{T_X(\Delta g(T_X,\sigma_X))^i}\right) \qquad (8)$$

where $K^{(i)}$ are constants and $\Delta g(T_X,\sigma_X)$ is the Gibbs free energy of crystallization.[11,27,30,35] The number $i = 2$, if the initial crystallization rate is controlled by the nucleation, and $i = 1$, if by the growth. We use here the WLF equation in order to reduce the number of fitting parameters

$$\phi(T,\sigma) = \exp\left(\frac{C_1^{WLF}(T - T_s)}{T - T_s + C_2^{WLF}}\right) \qquad (9)$$

where the "universal" constants $C_1^{WLF} = 8.86 \ln 10$ and $C_2^{WLF} = 101.6$ K, and a reference temperature $T_s = T_g + 50$ K[34] with the stress dependence of T_g shown in Figure 4a.

To properly estimate Δg, the difference between the equilibrium melting temperature $T_f^0(\sigma_f^0)$ and the observed melting one $T_f(\sigma_f)$ must be taken into account because $T_f^0(\sigma_f^0 = 0) - T_f(0)$ is expected to amount to about 50 K and much larger than the apparent supercooling $T_f - T \simeq 20$ K at high T_X (Figure 4a). We adopt the value of unvulcanized natural rubber, 35.5 °C, as $T_f^0(0)$ and assume the stress dependence of T_f^0 is the same as the present result: $T_f^0(\sigma_f^0) = 308.7 + 45\sigma_f^0$ K (σ_f^0 in MPa). If $T_f(\lambda)$ shown by the broken line in Figure 4b is shifted upward so that $T_f^0(\lambda_m = 1) = 35.5$ °C, $T_f^0(\lambda_m)$ is lower by about 8 K than the equilibrium melting temperature of natural rubber determined by the Hoffman−Weeks plot in the range from $\lambda = 2$ to $\lambda = 4$.[28,36] Further assumption $\Delta\hat{h}_f$ = constant = 64 MJ/m^3 leads to $\Delta s_f = 0.21$ MJ/(m^3 K) and $\Delta\lambda_f = 9.3$ by eq 5. The driving force for crystallization $\Delta g(T_X,\sigma_X)$ is given either by $\Delta g = \Delta s_f \Delta T$ with $\Delta T = T_f^0(\sigma_X) - T_X$ or by $\Delta g = \Delta\lambda_f\Delta\sigma$ with $\Delta\sigma = \sigma_f^0(T_X) - \sigma_X$, neglecting the variation in Δs_f and $\Delta\lambda_f$ with temperature and stress. In parts a and b of Figure 13, $\log \dot{\lambda}(T_X,\sigma_X) - \log \phi(T_X,\sigma_X)$ is plotted against $(T_X(\Delta g)^2)^{-1}$ and $(T_X\Delta g)^{-1}$, respectively.

The nucleation-controlled case ($i = 2$, Figure 13a) shows a better linear relation between $\log \dot{\lambda} - \log \phi$ and $(T_X(\Delta g)^2)^{-1}$ with the intercept $X_0^{(2)} = 1800$ s^{-1} and the slope $K^{(2)} = 1.6 \times 10^{18}$ J^2 K/m^6. With these values, the contour lines of $\dot{X}_{onset}(T_X,\sigma_X)$ are calculated by eqs 7−9 and shown in Figure 4a by the solid lines. Reproducibility of the experimental result is satisfactory. Accord-

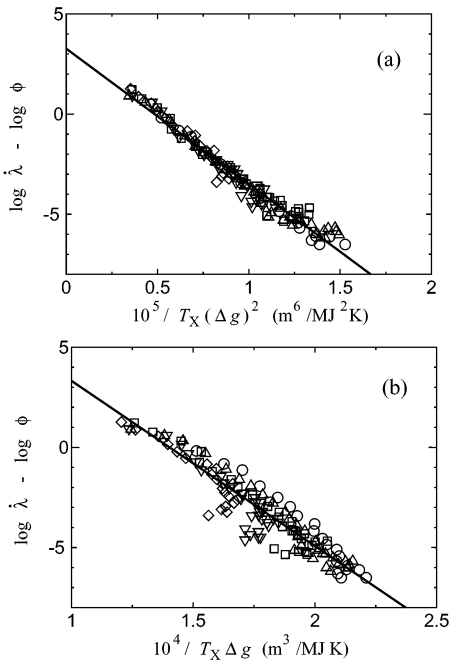

Figure 13. Examination of the kinetic factor for the results $T_X(\sigma_X,\dot{\lambda})$ shown in Figure 4 in the case that the initial crystallization rate is controlled (a) by the nucleation rate ($i = 2$) and (b) by the crystal growth rate ($i = 1$). The rates of deformation are (○) 0.0007, (△) 0.007, (□) 0.07, (▽) 0.7, and (◇) 7 s^{-1}.

ing to the classical nucleation theory,[35] the factor $K^{(2)}$ is given by $2C\sigma_s^2\sigma_e/k_B$, where C is a numerical factor determined by the shape of the nucleus, σ_s the surface tension of the lateral surface (the surface parallel to the chain axis) of the crystallite, σ_e the corresponding value for the end surface of the crystallite, and k_B Boltzmann's constant. We tentatively employ the values for the unvulcanized natural rubber determined by the melting and the crystallization analyses in the quiescent state: $\sigma_e = 2.4 \times 10^{-2}$ J m^{-2} [19,37,38] and $\sigma_s = 1.0$ or 1.4×10^{-2} J m^{-2}.[37,38] Then we obtain $K^{(2)} = 1.2 \times 10^{18}$ or 2.4×10^{18} J^2 K/m^6 with $C = 2\sqrt{\pi}$ for the cylindrical nucleus, corresponding to $\sigma_s = 1.0 \times 10^{-2}$ or 1.4×10^{-2} J m^{-2}, respectively. A fair coincidence is obtained between the observed and the calculated values.

The reproduction of the experimental results $f_{onset}(T_X,\sigma_X,\dot{\lambda}) = 0$ in Figure 4a apparently without any arbitrary parameter shows that reasonable are the present interpretation of the crystallization and the melting from the stress−strain−temperature measurements and the method of analysis. It may not be safe to conclude that the onset of crystallization observed in this study is controlled by the nucleation, when considering the assumptions and the approximations employed. However, the linear relation seen in Figure 13a and the agreement of its slope with the calculated value of $K^{(2)}$ suggest that the nucleation-controlled onset of crystallization is the case and that the thermodynamic quantities of polyisoprene are little affected by vulcanization and between natural and synthetic rubbers, since all the values used for $T_f^0(\sigma_f^0 = 0)$, $\Delta h_f(0)$, σ_e, and σ_s are borrowed from those of the unvulcanized natural rubber. The remarkable difference in crystallization rate among natural and synthetic rubbers with various vulcanization conditions[1,2,7,10,15] and with various contents of fatty acids and esters[17,18] may be attributable to the difference in the segmental mobility and in the

number of nucleation sites. For further investigation on the crystallization kinetics, awaited are the morphological studies on the crystallite and the measurement of the growth rate of the cross-linked rubbers.

In summary, the melting and the crystallization of isoprene rubber were studied by the measurements of the stress−strain−temperature relation under uniaxial deformation. The rise in melting temperature with stress is mainly attributed to the work of contraction upon melting. The simplified kinetic model can reproduce the relation between the temperature and the nominal stress at the onset of crystallization. The experimental method and the procedure of the analysis are presented to extract the information on the crystallization and the melting of rubber under strain from the thermoelastic measurements.

Acknowledgment. The authors thank Dr. R. Ohara of Toyo Tire & Rubber Co. Ltd. for kindly supplying the material. This work is partly supported by a Grant-in-Aid for Scientific Research from Japan Society for the Promotion of Science and from the Ministry of Education, Culture, Sports, Science and Technology of Japan.

References and Notes

(1) Gent, A. N.; Kawahara, S.; Zhao, J. *Rubber Chem. Technol.* **1998**, *71*, 668.
(2) Toki, A.; Fujimaki, T.; Okuyama, M. *Polymer*, **2000**, *41*, 5423.
(3) Valladares, C.; Sen, T.; Cakmak, M.; Toki, S. *International Conference on Flow Induced Crystallization of Polymers*, Salerno, Italy, 2001; p 169.
(4) Murakami, S.; Senoo, K.; Toki, S.; Kohjiya, S. *Polymer* **2002**, *43*, 2117.
(5) Toki, S.; Sics, I.; Ran, S.; Liu, L.; Hsiao, B. S.; Murakami, S.; Senoo, K.; Kohjiya, S. *Macromolecules* **2002**, *35*, 6578.
(6) Treloar, R. G. *The Physics of Rubber Elasticity*, 3rd ed.; Clarendon Press: Oxford, 1975.
(7) Toki, S.; Sics, I.; Ran, S.; Liu, L.; Hsiao, B. S. ACS Meeting, Rubber Division, 2002; paper no. 85.
(8) Miyamoto, Y.; Fukao, K.; Yamao, H.; Sekimoto, K. *Phys. Rev. Lett.* **2002**, *88*, 225504.
(9) Mitchell, G. R. *Polymer* **1984**, *25*, 1562.
(10) Gent, A. N. *Trans Faraday Soc.* **1954**, *50*, 521.
(11) Kim, H.-G.; Mandelkern, L. *J. Polym. Sci., Part A-2* **1968**, *6*, 181.
(12) Göritz, D.; Müller, F. H.; Sietz, W. *Prog. Colloid Polym. Sci.* **1977**, *62*, 114.
(13) Luch, D.; Yeh, G. S. Y. *J. Appl. Phys.* **1972**, *43*, 4326; *J. Macromol. Sci., Phys.* **1973**, *B7*, 121; *J. Polym. Sci., Polym. Phys. Ed.* **1973**, *11*, 467.
(14) Strobl, G. *The Physics of Polymers*; Springer-Verlag: Berlin, 1996; Chapter 4.
(15) Bekkedahl, H.; Wood, L. A. *Ind. Eng. Chem.* **1941**, *33*, 381.
(16) Bruzzone, M.; Mazzei, A.; Giuliani, G. *Rubber Chem. Technol.* **1974**, *47*, 1175.
(17) Kawahara, S.; Nishiyama, N.; Kakubo, T.; Tanaka, Y. *Rubber Chem. Technol.* **1996**, *69*, 600.
(18) Nishiyama, N.; Kawahara, S.; Kakubo, T.; Hwee, E. A.; Tanaka, Y. *Rubber Chem. Technol.* **1996**, *69*, 608.
(19) Dalal, E. N.; Taylor, K. D.; Phillips, P. J. *Polymer* **1983**, *24*, 1623.
(20) Roberts, D. E.; Mandelkern, L. *J. Am. Chem. Soc.* **1955**, *77*, 781.
(21) Kim, H.-G.; Mandelkern, L. *J. Polym. Sci., Part A-2* **1972**, *10*, 1125.
(22) Greene, A.; Ciferri, A. *Kolloid Z. Z. Polym.* **1962**, *186*, 1.
(23) Mark, J. E. *Rubber Chem. Technol.* **1975**, *48*, 495.
(24) Krigbaum, W. R.; Roe, R.-J. *J. Polym. Sci., Part A* **1964**, *2*, 4391.
(25) Göritz, D.; Grassler, R. *Rubber Chem. Technol.* **1987**, *60*, 217.
(26) Flory, P. J. *J. Chem. Phys.* **1947**, *15*, 397.
(27) Gent, A. N. *J. Polym. Sci., Part A* **1965**, *3*, 3787.
(28) Krigbaum, W. R.; Dawkins, J. V.; Via, G. H.; Balta, Y. I. *J. Polym. Sci., Part A-2* **1966**, *4*, 475.
(29) Gent, A. N. *J. Polym. Sci., Part A-2* **1966**, *4*, 447.
(30) Hoffman, J. D.; Davis, G. T.; Lauritzen, J. I., Jr. In *Treatise on Solid State Chemistry*; Hannary, N. B., Ed.; Plenum: New York, 1976; Vol. 3, Chapter 7.
(31) Miyamoto, Y.; Tanzawa, Y.; Miyaji, H.; Kiho, H. *Polymer* **1992**, *33*, 2496.
(32) Miyaji, H.; Miyamoto, Y.; Taguchi, K.; Hoshino, A.; Yamashita, M.; Sawanobori, O.; Toda, A. *J. Macromol. Sci.* **2003**, *B42*, 867.
(33) Wilson, H. A. *Philos. Mag.* **1900**, *50*, 238.
(34) Williams, M. L.; Landel, R. F.; Ferry, J. D. *J. Am. Chem. Soc.* **1955**, *77*, 3701.
(35) Lauritzen, J. I., Jr.; Hoffman, J. D. *J. Res. Natl. Bur. Stand. (U.S.)* **1960**, *64A*, 73.
(36) It is not justified to compare $T_f(\lambda)$ of rubbers prepared under different vulcanization conditions without referring to the cross-link density. In our preliminary experiments, however, the effect of the cross-link density on $T_f(\lambda)$ is relatively small, and hence $T_f(\sigma)$ depends on the cross-link density according to the elastic modulus of the rubber.
(37) Edwards, B. C. *J. Polym. Sci., Polym. Phys. Ed.* **1975**, *13*, 1387.
(38) Phillips, P. J.; Vatansever, N. *Macromolecules* **1987**, *20*, 2138.

MA0342877